World Journal of Pharmaceutical Science and Research
www.wjpsronline.com
Research Article
ISSN: 2583-6579
SJIF Impact Factor: 3.454
Year - 2024
Volume: 3; Issue: 2
Page: 38-53

EFFECTS OF THE ADRENERGIC BLOCKERS TAMSULOSIN AND CARVEDILOL ON THE HOMEOSTASIS OF THE ENDOPLASMIC RETICULUM OF LIVER CELLS

Juan Carlos Rivera-Navarro[1], Mariana Yazmin Medina Pizaño[2], Sandra Luz Martínez-Hernández[3], Javier Ventura-Juárez[4], David Ibarra-Martínez[5] and Martín Humberto Muñoz-Ortega[*5]

[1]Department of Medicine, Center of Health Sciences, Autonomous University of Aguascalientes, Aguascalientes, 20100 Mexico.
[2]Faculty of Medicine, Department of Histology, Autonomous University of Nuevo Léon, Monterrey, Nuevo León, 64460, Mexico.
[3]Department of Microbiology, Center of Basic Sciences, Autonomous University of Aguascalientes, Aguascalientes, 20100 Mexico.
[4]Department of Morphology, Center of Basic Sciences, Autonomous University of Aguascalientes, Aguascalientes, 20100 Mexico.
[5]Department of Chemistry, Center of Basic Sciences, Autonomous University of Aguascalientes, Aguascalientes, 20100 Mexico.

Article Received: 10 January 2024 | | ***Article Revised: 31 January 2024*** | | ***Article Accepted: 20 February 2024***

Corresponding Author: Martín Humberto Muñoz-Ortega
Department of Chemistry, Center of Basic Sciences, Autonomous University of Aguascalientes, Aguascalientes, 20100 Mexico.
DOI: https://doi.org/10.5281/zenodo.10940616

ABSTRACT

Carvedilol and tamsulosin, both belonging to the family of adrenergic receptor antagonists, have been proposed in multiple recent studies (both in vitro and in vivo) for the treatment of liver and kidney fibrosis. However, there are reports of possible side effects that contradict its therapeutic properties in chronic liver damage. Furthermore, there is insufficient toxicological information on these drugs to ensure their safety. The present study investigates the signaling pathways activated during endoplasmic reticulum stress using a cell model derived from hepatocytes. Our MTT assay results suggest that both drugs reduce cell viability in a time-dependent manner, with a tendency for proliferation at higher concentrations. The study of gene expression kinetics for UPR markers revealed a moderate response in the PERK-ATF4 and IRE1-XBP1 branches after 12 hours of treatment. GRP78 showed an increase in expression within the initial hours of treatment; however, no significant differences in its synthesis were observed when evaluated with Western blot. Finally, the study found that tamsulosin did not alter the rate of protein synthesis, while carvedilol briefly reduced it. Our findings suggest that both carvedilol and tamsulosin upregulate genes associated with the response to misfolded proteins, but this alone is insufficient to trigger the cell death response.

KEYWORDS: Carvedilol, Tamsulosin, Reticular stress, HepG2 Cells, Safety.

INTRODUCTION

The Adreno-blockers are a group of pharmacological agents that inhibit the activity of the sympathetic nervous system by binding to the same receptors as catecholamines, without triggering their physiological response. [1] These blockers are classified into three main categories: α1, α2, and β, with further subtypes within each category, based on their amino acid sequence, ligand affinity, and signal transduction.[2] They belong to the extensive family of G protein-coupled receptors, which are distributed throughout the body.[3] These receptors play a crucial role in hemodynamic regulation, body temperature, and metabolism.[1]

Tamsulosin, a sulfonamide, selectively blocks α1 type adrenergic receptors, exhibiting an antagonistic effect on α1A and α1D receptors and functioning as an inverse agonist on α1B receptors.[4–6] It is widely utilized for treating lower urinary tract symptoms (LUTS) associated with benign prostatic hyperplasia and bladder obstructions.[7]

Carvedilol, an aryl ethanolamine, blocks β1, β2, and α1 adrenergic receptors.[8] It is used to treat heart failure, hypertension, and heart attacks.[9] as well as portal hypertension resulting from ascites, a common complication in cirrhotic patients.[10] Clinical studies have demonstrated its efficacy in primary and secondary prophylaxis against variceal bleeding.[11] Carvedilol also contains a carbazole group in its structure, which is attributed to its antioxidant and cardioprotective properties.[9]

The use of adrenoblockers has recently been suggested for the treatment of hepatic fibrosis because they target the receptors expressed by hepatic stellate cells, inhibiting their activation and contributing to the liver healing process.[12] Several animal studies involving liver lesions treated with adrenergic antagonists have demonstrated improvements compared to control groups.[13–16]

Despite FDA approval since the 1990s and ongoing research into novel applications, there is a lack of information regarding the isolated toxicological effects on liver parenchymal cells. Both drugs are metabolized by the cytochrome P450 multienzyme system, primarily located in hepatocyte subcellular membranes.[7,9,17] These drugs are contraindicated in patients with liver failure because their chemical substances or derived metabolites can disrupt cellular homeostasis and exacerbate health problems due to their toxicity.[18,19] The role of the endoplasmic reticulum in the pathophysiology of various liver diseases, including hepatitis, fatty liver, and drug-induced hepatotoxicity, has recently gained recognition. It plays essential roles in the cell, including lipid biosynthesis, calcium storage, and the processes of protein synthesis, folding, assembly, trafficking, post-modification, and quality control.[20]

Oxidative stress, hypoxia, energy depletion, xenobiotic interactions, or disruptions in cellular homeostasis can initiate failures in endoplasmic reticulum quality control, affecting protein folding and disposal.[21] To mitigate these impaired functions, cells activate the unfolded protein response (UPR), a survival mechanism triggered by persistent stress. However, prolonged UPR activation can ultimately lead to programmed cell death.[22]

This response depends on three interconnected branches that activate when uncoupled from GRP78, a resident chaperone protein of the endoplasmic reticulum. These transmembrane sensors are PERK (double-stranded RNA-activated ER protein kinase), ATF6 (Activating Transcription Factor 6), and IRE1 (Inositol-dependent enzyme 1).[23]

PERK dimerizes and autophosphorylates, which subsequently phosphorylates the eukaryotic initiation factor eIF2. This phosphorylation event inhibits general protein synthesis while allowing the translation of select proteins, such as ATF4.

ATF4 then translocates to the nucleus and induces the transcription of genes necessary to restore homeostasis.

ATF6, on the other hand, is activated through proteolysis following its translocation from the ER to the Golgi apparatus. The 50 kDa fraction on the cytosolic side is also translocated to the nucleus to stimulate gene expression. Finally, IRE1 is activated through oligomerization and autophosphorylation. Its endonuclease domain eliminates an intron from the XBP1 mRNA, encoding a functional protein that acts as a transcription factor for stress response genes.[24]

Considering the evidence supporting the use of carvedilol and tamsulosin adrenoblockers in the treatment of chronic liver damage processes, it's crucial to investigate whether these drugs can induce cell damage that hinders liver recovery. Therefore, we will evaluate the potential activation of a stress response in the endoplasmic reticulum of HepG2 cells, serving as a model for liver parenchyma cells, when interacting with carvedilol and tamsulosin.

Experimental Procedures

Cell culture

HepG2 human hepatocellular carcinoma cells were obtained from the UANL histology laboratory and cryopreserved until use. Upon thawing, cells underwent at least two sub-culturing steps before experimental use. All cells were cultured following the manufacturer's instructions, using DMEM (Corning, 10-090-CV) supplemented with 2% fetal bovine serum (FBS), 2% L-glutamine (Corning, 25-005-CI), and 1% penicillin, streptomycin, and amphotericin B (Sigma, A5955) at 37°C in a humidified atmosphere containing 5% CO_2.

Treatments with carvedilol and tamsulosin

A stock solution of carvedilol (Sigma, PHR1265) and tamsulosin (Sigma, T1330) was prepared at a concentration of 50 mM in DMSO. From this solution, preset treatments at concentrations of 0.01 µM, 0.1 µM, 1 µM, and 10 µM were obtained using complete DMEM medium as the solvent.

MTT assay

The cells were seeded in 96-well plates at a density of 1 × 104 cells per well and incubated for 24 hours. When the cellular confluency reached 75%, the medium was replaced with a treatment containing 0.01 µM, 0.1 µM, 1 µM, and 10 µM of the α/β adrenoreceptor antagonists for 24, 48, and 72 hours. After the respective incubation periods, a cell viability assay was conducted following the protocol by Mosmann (1983). The treatment was replaced with a complete culture medium containing 0.5 mg/ml of diluted MTT (Sigma, M2128) and incubated for 4 hours at 37°C. Subsequently, the culture medium was removed, and the formazan crystals were dissolved in 150 µL of acid isopropanol (0.1 N HCl in isopropanol). After shaking at 200 rpm for 10 minutes, MTT reduction was quantified by measuring the absorbance of light at 595 nm with a reference filter set at 655 nm using the iMark Microplate Reader (BioRad, California, USA).

Isolation of total RNA and reverse transcription-quantitative polymerase chain reaction (RT-qPCR)

HepG2 cells were cultured in 6-well plates at a density of 2.5×10^5 cells per well and incubated for 24 hours. When cellular confluency reached 75%, they were treated with 0.01 µM, 0.05 µM, and 0.1 µM of the α/β adrenoreceptor antagonists for 4, 8, 12, and 24 hours. As a positive control for endoplasmic reticulum stress, 5 µg/ml Tunicamycin (Sigma, T7765) was used, following the protocol proposed by Abdullahi et al. (2017).[25]

Total RNAs were extracted using the Direct-zol RNA Miniprep kit (Zymo Research, R2050-R2053) following the manufacturer's instructions, quantified using a Biodrop (Isogen life Science, Barcelona, España), and stored at -80°C.

Reverse transcription was performed with 1 µg of total RNA using the RevertAid First Strand cDNA Synthesis Kit (K1621, Thermo Scientific, Waltham, MA, USA). Subsequently, real-time quantitative PCR was carried out using the Maxima SYBR Green/ROX qPCR Master Mix (2X) (K0221, Thermo Scientific, Waltham, MA, USA) on a StepOne apparatus (Applied Biosystems) with the following cycling conditions: 50°C for 2 min, 95°C for 45 sec, followed by 40 cycles of 95°C for 45 sec and 60°C for 45 sec. The oligonucleotides listed in table 1 were designed with information and tools available on the NCBI page.[26,27] Relative expression ratios were normalized to 18S rRNA as the internal housekeeping gene, and differences were determined using the 2-ΔΔCt method.[28]

Puromycin analysis

The measurement of protein synthesis in cultured cells using western blotting was based on the protocol by Ravi et al. (2020) In brief, HepG2 cells were cultured in 6-well plates at a density of 2.5×10^5 cells per well and incubated for 24 hours. After 12 hours of stimulation with 0.01 µM of the α/β adrenoreceptor antagonists, the supplemented culture medium was replaced with a medium containing 1 µM of Puromycin (Tocris Bioscience, 4089). After 15 minutes, excess puromycin was removed by washing with a 0.00036% Digitonin (Sigma, D141) PBS solution. A positive control using homoharringtonine (Sigma, SML1091) at 50 mM/9h was employed. Subsequently, total protein extraction and the western blot protocol were followed.[29]

Protein extraction and Western Blot

To analyze the expression of GRP78 and LC3A/B proteins in HepG2 cells, HepG2 cells were cultured in 6-well plates at a density of 2.5×10^5 cells per well and incubated for 24 hours. Cells were treated with 0.01 µM of α/β adrenergic receptor antagonists for 12 hours. Tunicamycin (5 µg/ml) was used as a positive control for endoplasmic reticulum stress. Cell lysates were prepared by lysing cells in RIPA buffer with 1% protease inhibitors and then centrifuged at 14,000 x g for 15 minutes at 4°C. Protein concentration was determined using the BCA method with the Pierce kit. Each protein extract was separated on a 10% SDS-polyacrylamide gel and then transferred to PVDF membranes. Thirty micrograms of protein extract were loaded for the detection of GRP78 and LC3A/B. Membranes were blocked for 2 hours at room temperature with TBST containing 5% non-fat milk. Specific antibodies for GRP78, LC3A/B, GAPDH, and BiP were used to detect the proteins of interest. Incubations with the corresponding antibodies were carried out overnight. After immunodetection and densitometric analysis, membranes were washed and incubated again with antibodies for normalization. Secondary antibodies conjugated with HRP were used for protein detection. Transfers were visualized using an ECL substrate kit and a transfer scanner. Protein band quantification was performed using ImageJ software.

Scanning electron microscopy

HepG2 cells were analyzed by scanning electron microscopy to observe the morphological changes upon treatment with 0.01 µM of α/β adrenergic receptor antagonists for 12 hours. A total of 10^5 cells grown on coverslips in 24-well plates were fixed in 2.5% glutaraldehyde for 10 min at 25 °C. The samples were washed with distilled water and dehydrated before being placed on a critical point dryer for 30 min (IR Chamber Scope). Then, the mounted of the sample was carried out. Finally, the samples were plated with gold in Denton Vacuum before observing them with a scanning electron microscope (JEOL JSM-5900 Low Vacuum SEM, Japan).

Statistical Analysis

Statistical analysis was conducted using Microsoft Excel and GraphPad Prism 9 software. The results were presented as the mean ± SEM. The Shapiro-Wilk normality test, analysis of variance (ANOVA), and Dunnett's post hoc test were used for multiple comparisons. P-values less than 0.05 were considered significant and indicated by asterisks as follows: *p < 0.05, **p < 0.01, ***p < 0.001, ****p < 0.0001.

RESULTS

Cytotoxic assessment of α/β adrenoreceptor antagonists in HepG2

In the case of carvedilol, a cytotoxic effect on HepG2 cells is observed with longer interaction times and lower concentrations. At 24 hours, no significant changes were observed in the metabolic activity of the treated cells at different concentrations of this drug. However, after 48 hours, the activity notably decreased in all doses. In the group treated with 0.01 µM, the difference was statistically significant (73.69±5.63%).

Similar to the previous case, at 72 hours, the most negative effects were recorded at the lowest concentrations. All groups showed significant differences with values of 66.84 ± 4.31%, 76.13 ± 4.55%, 81.41 ± 4.52%, and 79.27 ± 3.94% for 0.01 µM, 0.1 µM, 1 µM, and 10 µM, respectively. It is observed that as the exposure time of the cells to the drug increases, cell viability decreases with respect to its control, regardless of the concentration (Figure 1A).

When the cells were treated with tamsulosin, a very similar behavior was observed. At 24 hours, it had no effect on the percentage of cell viability at the study concentrations. However, after 48 hours, a decrease in viability was seen at the lowest concentrations. The groups treated with 0.01 µM and 0.1 µM had values of 70.00 ± 4.69% and 83.26 ± 4.02%, respectively.

At 72 hours, all concentrations had a statistically significant effect on the cells, except for the highest concentration (10 µM), which did not show differences from the control. The values were 72.19 ± 3.42%, 81.79 ± 3.79%, and 87.49 ± 2.46% for the groups of 0.01 µM, 0.1 µM, and 1 µM, respectively (Figure 1B).

Effects of carvedilol and tamsulosin on expression and synthesis of GRP78

In the kinetic study of gene expression of GRP78, treatment with carvedilol (Figure 2A) showed an overexpression within the first 4 hours at all three concentrations studied, with the most significant increase observed at the lowest concentration of 0.01 µM. This overexpression was comparable to the positive control of tunicamycin (5.94 ± 0.03 and 6.05 ± 0.97, respectively). As time passed, the expression became regulated; however, at 12 hours, a significant difference was still observed with the concentration of 0.01 µM (2.70 ± 0.08).

On the other hand, the tamsulosin group (Figure 2B) exhibited significant overexpression within the first few hours of treatment, especially with the higher doses. At 4 hours, with 0.05 µM, it was expressed up to 6.69 ± 0.99 times compared to the negative control, and with 0.1 µM, it was 6.38 ± 0.93 times. This behavior lasted until 8 hours, with 7.46 ± 1.95 and 5.82 ± 1.16 times, respectively. At the lowest concentration (0.01 µM) of tamsulosin, there were no statistically significant effects, and the expression levels remained between 1.61 and 3.08.

The synthesis of the GRP78 protein did not differ significantly between the control, carvedilol, and tamsulosin treated groups. The control group had a mean of 0.053 ± 0.009 units relative to GAPDH, the group treated with tamsulosin had

0.073 ± 0.025 units, and carvedilol had 0.034 ± 0.008 units. In contrast, the interaction with tunicamycin (TM) triggered a significant increase in the expression of this marker, up to 0.869 ± 0.104 units (Figure 2C-D).

Gene expression kinetics of PERK-ATF4 branch.

Carvedilol did not show statistically significant differences in PERK mRNA levels at the times and concentrations considered in the study (Figure 3A). However, statistical analysis revealed that at 12 hours with 0.01 µM, ATF4 mRNA production almost doubled (1.90 ± 0.14), similar to the positive control with TM (2.30 ± 0.03) (Figure 3C).

In contrast, tamsulosin-treated cells only exhibited a response at 12 hours at the lowest concentration (0.01 µM), with 2.70 ± 0.82 times more PERK mRNA than the negative control (Figure 3B). Consistently, activating transcription factor 4 also showed a significant increase of 1.46 ± 0.01 under the same conditions (Figure 3D).

Gene expression kinetics of IRE-XBP1 branch.

In the carvedilol group (Figure 4A), a significant increase in the expression of IRE1α is observed within the first 4 hours with 0.1 µM, similar to the positive control group (1.56 ± 0.29). An overexpression is also noted after 12 hours of treatment with the concentration of 0.01 µM, showing a 2.51 ± 0.10-fold increase compared to the negative control.

The groups treated with tamsulosin (Figure 4B) exhibit a very similar behavior to carvedilol: statistical differences are present at 4 hours in the 0.05 µM group (1.53 ± 0.05), after 8 hours with 0.1 µM (2.54 ± 0.45), and at 12 hours with 0.01 µM (2.54 ± 0.45).

In the carvedilol group (Figure 4C), the expression of mRNA encoding for XBP1 showed statistical significance within the first 4 hours at concentrations of 0.05 µM and 0.01 µM, with levels of 2.36 ± 0.29 and 2.39 ± 0.10, respectively. An overexpression is observed again at 12 hours with 0.01 µM, reaching 2.89 ± 0.24.

The tamsulosin-treated group (Figure 4D) exhibited elevated levels within the first 4 hours at a concentration of 0.05 µM (2.58 ± 0.34) and with 0.01 µM after 12 hours of interaction (2.49 ± 0.39).

Carvedilol and tamsulosin do not alter the ratio of LC3-I/LC3-II

The expression of microtubule-associated proteins 1A/1B and 3B light chain, which are associated with early steps in autophagosome formation, was measured. The ratio of LC3A/B-I to LC3A/B-II did not exhibit statistically significant changes between the groups treated with carvedilol and tamsulosin (Figure 5 A and B). The positive control with tunicamycin showed an upward trend with 0.811 ± 0.416 relative units, but it was not statistically significant either.

Ultrastructural effects of tamsulosin and carvedilol on HepG2 cells

HepG2 cells showed time-and dose-dependent changes with treatment of tamsulosin and carvedilol. At 12 h post-treatment, pro-apoptotic cells (asterisk) (exhibiting cell shrinkage morphology) as well as cells with cytoplasmic contraction (arrow), nuclear condensation, and shedding among adjacent cells (#) were observed in the treatment with tunicamycin (Figure 5C). Cells exposed carvedilol doses 0.01 µM presented features such as, cytoplasmic contraction with appearance of irregularities on the cell surface (arrow), cell fragmentation, and the appearance of apoptotic bodies (asterisk) (Figure 5C). However, when cells were exposed to tamsulosin 0.01 µM the morphology did not show differences between the treated and control cells and presented a normal nucleus, indicating the no onset of apoptosis or necrosis (Figure 5C).

Protein synthesis rate assessment with puromycin

The control group with puromycin pretreatment had a value of 7.92 ± 1.15 relative units, while the group with normal proteins without pretreatment had a value of 1.98 ± 0.23. The difference was statistically significant with p=0.0004 (Figure 6A). The group treated with the pentacyclic alkaloid HHT exhibited a very low protein synthesis rate compared to the control, with 1.83 ± 0.17 relative units, which is very similar to the group without puromycin pretreatment. The adrenergic blockers did not show statistically significant differences (p=0.3064) compared to the puromycin-treated control group. However, the significance levels differ when compared to the HHT group. The group treated with tamsulosin showed levels of 8.31 ± 1.21 with p=0.0005, which are slightly higher than the control with normal protein synthesis rates. In contrast, the group treated with carvedilol had levels of 6.50 ± 0.35 with p=0.0056.

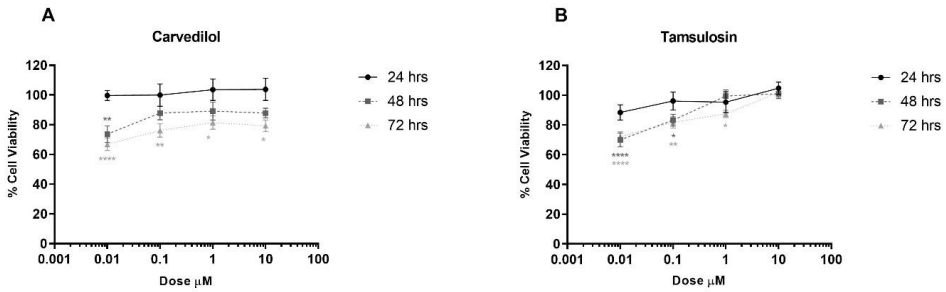

Figure 1: Effects of carvedilol and tamsulosin on the viability of hepg2 cells at different times and concentrations.

Cell viability represented in percentages is on the Y axis, the X axis represents the doses on a logarithmic scale. Each point represents the mean ± SEM and has 12 observations (n = 12). Asterisks indicate the level of significance; * p <0.05, ** p <0.01, *** p <0.001, **** p <0.0001.

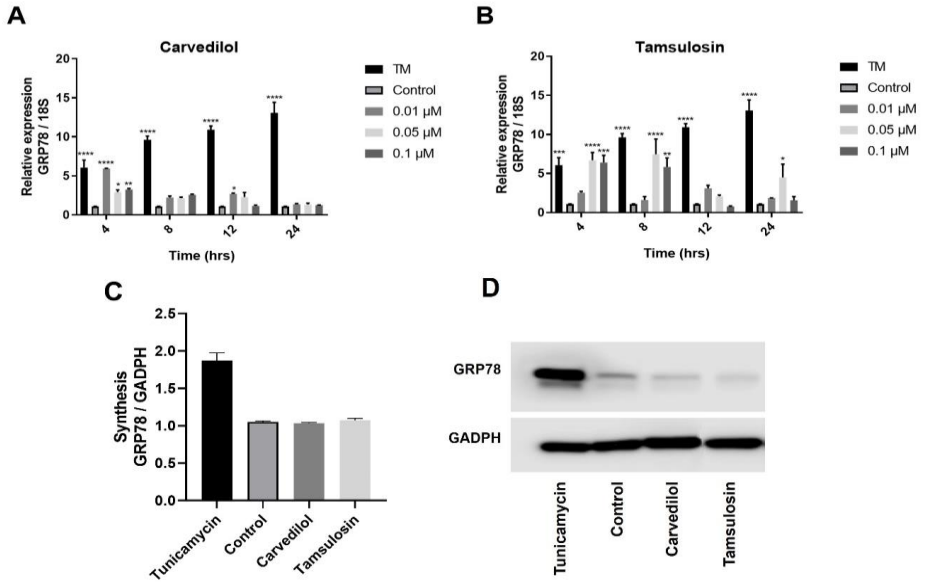

Figure 2: Effects of carvedilol and tamsulosin in HepG2 cells on the expression and synthesis of GRP78.

HepG2 cells interacted with 0.01, 0.05 and 0.1 µM of (A) carvedilol and (B) tamsulosin for a period of 4, 8, 12 and 24 hours, and evaluated the expression of GRP78 by RT q PCR (n=3). (C-D) GRP78 was subsequently detected by western blot after 12 h of interaction with 0.01 µM carvedilol and tamsulosin. The results were analyzed by

densitometry with Image J software and normalized with GADPH (n=4),. Multivariate statistical analyzes ANOVA with Dunnett's post hoc were performed. Asterisks indicate the level of significance; *p<0.05, **p<0.01, ***p<0.001, ****p<0.0001. TM: Tunicamycin.

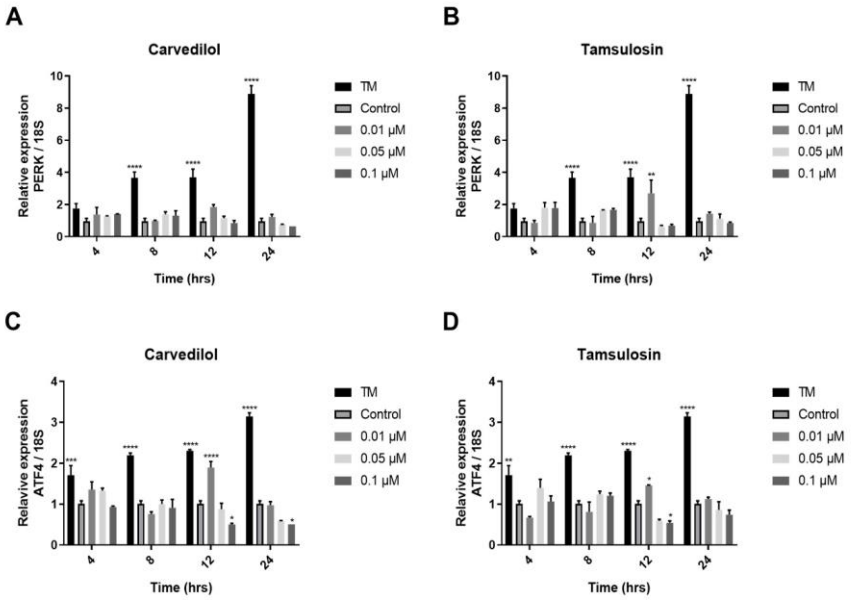

Figure 3: Kinetics of gene expression of PERK-ATF4 branch.

PERK expression was evaluated with 0.01, 0.05 and 0.1 µM treatments of (A) carvedilol and (B) tamsulosin at 4, 8, 12 and 24 hrs. Subsequently, the expression of ATF4 was evaluated under the same conditions; (C) carvedilol treated group, (D) tamsulosin treated group. Each group has three observations (n=3) and is represented as the mean ± standard deviation of the mean. Two-way ANOVA with Dunnett's post hoc statistical analysis was performed. Asterisks indicate the level of significance; * p<0.05, **p<0.01, ***p<0.001, ****p<0.0001. TM: Tunicamycin.

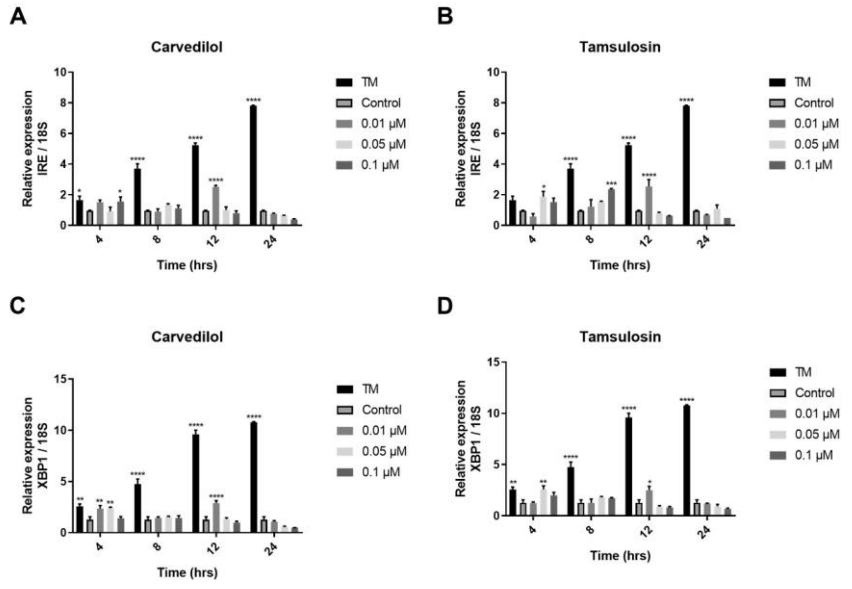

Figure 4: Kinetics of gene expression of IRE-XBP1 branch.

IRE1 expression was evaluated with 0.01, 0.05 and 0.1 µM treatments of (A) carvedilol and (B) tamsulosin at 4, 8, 12 and 24 hrs. Subsequently, the expression of XBP1 was evaluated under the same conditions; (C) carvedilol treated group, (D) tamsulosin treated group. Each group has three observations (n=3) and is represented as the mean ± standard deviation of the mean. Two-way ANOVA with Dunnett's post hoc statistical analysis was performed. Asterisks indicate the level of significance; * p<0.05, **p<0.01, ***p<0.001, ****p<0.0001. TM: Tunicamycin.

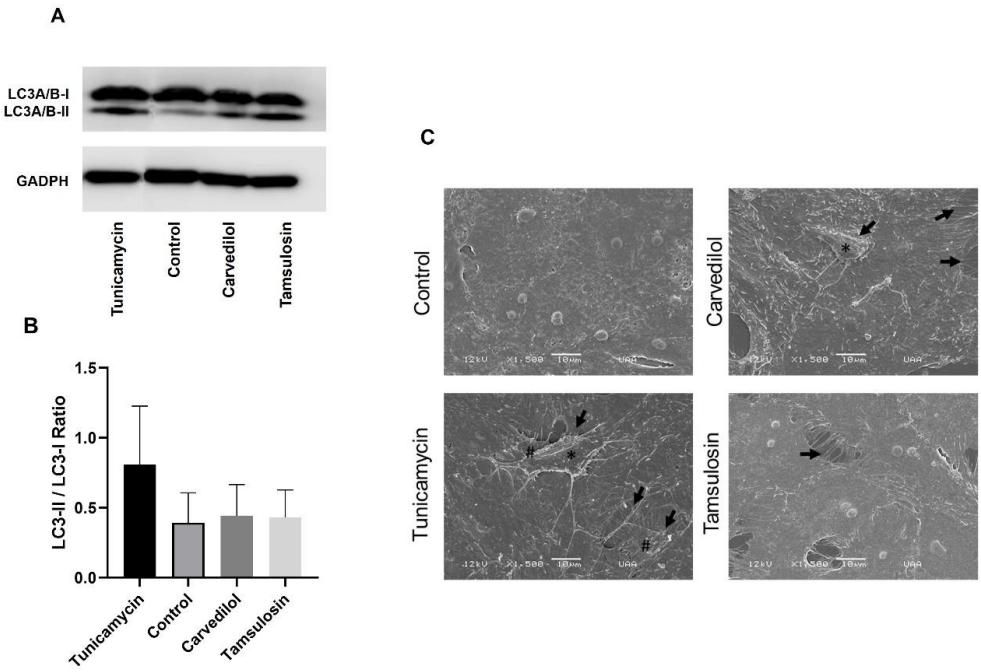

Figure 5: Effects of drug treatments on LC3A/B expression and Ultrastructural effects.

A) A photograph of a PVDF membrane developed with a chemiluminescence treatment is observed, where the upper band corresponds to LC3-I and the thinnest below is LC3-II. B) The ratio of LC3-II to LC3-I in each sample is presented. The results were analyzed by densitometry with Image J software and normalized with glyceraldehyde-3-phosphate dehydrogenase (GADPH). Each group has 4 repetitions (n=4), the graph represents the means with error bars and the standard deviation of the means. In all cases there was a normal distribution, and the assumption of homoscedasticity was met. A one-way ANOVA with Dunnett's post hoc was performed. Asterisks indicate the level of significance: * p<0.05, **p<0.01, ***p<0.001, ****p<0.0001. C) Ultrastructural effects of tamsulosin and carvedilol on HepG2 cells. At 12 h post-treatment, pro-apoptotic cells (asterisk) (exhibiting cell shrinkage morphology) as well as cells with cytoplasmic contraction (arrow) and shedding among adjacent cells (#) were observed in the treatment with tunicamycin. Cells exposed carvedilol doses 0.01 µM presented cytoplasmic contraction with appearance of irregularities on the cell surface (arrow). However, when cells were exposed to tamsulosin 0.01 µM the morphology did not show differences between the treated and control cells.

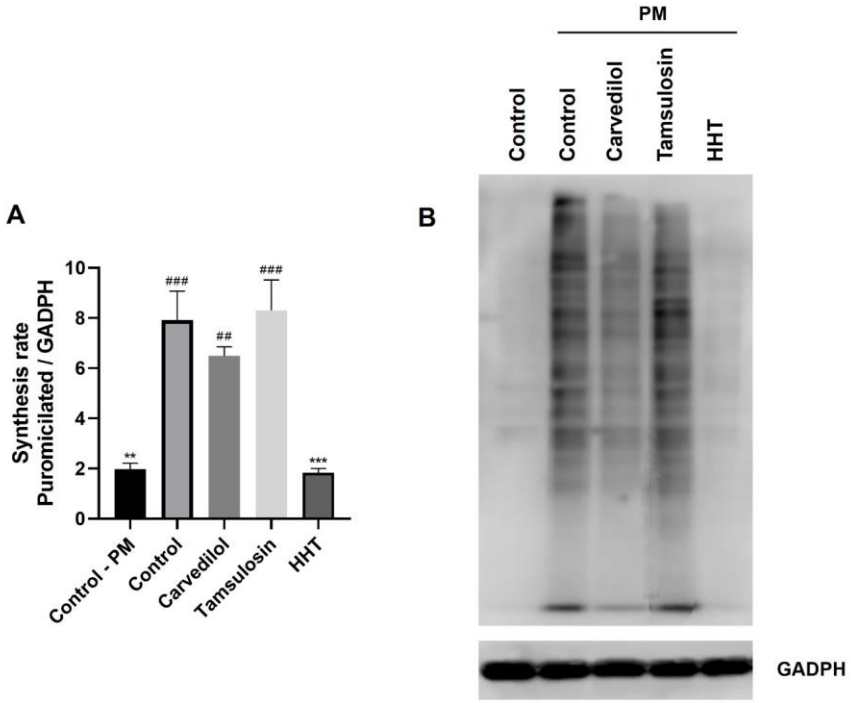

Figure 6: Effects of drug treatments on global protein synthesis.

A) Western blot membrane photograph of the protein synthesis experiment revealed by chemiluminescence. 1: Control without puromycin, 2: Control with puromycin, 3: Carvedilol, 4: Tamsulosin, 5: HHT. B) Graph derived from the densitometric analysis of the PVDF membranes. Results were analyzed with Image J software and normalized with housekeeping GADPH. Each group has 3 repetitions (n=3), the graph represents the means with the standard deviation of the mean. In all cases, there was a normal distribution, and the assumption of homoscedasticity was met. A one-way ANOVA with Dunnett's post hoc was performed: Asterisks indicate differences concerning Control with puromycin (*), numerals are for control treated with HHT (#); * $p<0.05$, ** $p<0.01$, *** $p<0.001$, **** $p<0.0001$.

DISCUSSION

The concentrations of 0.01 to 0.1 µM for both drugs helped us identify the time and concentration at which the drugs can induce the UPR. In this study, evidence has been presented that neither tamsulosin nor carvedilol induces the unfolded protein response. Carvedilol, at therapeutic doses in human patients, exhibits a maximum serum concentration in the range of 0.01 to 0.1 µM, with a half-life of 7 to 10 hours.[30] Similarly, tamsulosin has a serum concentration of approximately 0.01 µM, with a half-life of 9 to 13 hours.[7]

The observations recorded in the tamsulosin cytotoxicity assays align with observations reported by various authors using different cell lines. According to studies conducted by Forbes et al. (2016), some alpha-blockers exhibit anticancer properties independent of their therapeutic effects in patients. Their cytotoxicity studies, using resazurin, reveal that tamsulosin has the least cytotoxic effect on PC-3 and LNCap prostate cancer cell lines, while Doxazosin and prazosin exhibited greater cytotoxic effects in all cases.[31] These effects are attributed to the quinazoline ring in Doxazosin´s structure, which can activate cell death mechanisms. This mechanism may involve cellular targets such as the activation of caspases 8/3, VEGF, EGFR, HER2/Neu, or topoisomerase.[32] On the other hand, tamsulosin and silodosin showed no significant effects on cell viability even after 72 hours of continuous treatment at the highest concentration of 100 µM.

Other studies indicate that ACHN and Caki-2 kidney cancer cell lines, when treated with 50 µM tamsulosin, exhibited no significant changes compared to naftopidil. In contrast, naftopidil inhibited proliferation by inducing G1 cell cycle arrest.[33] Another study by Forbes et al. reports on the cytotoxicity of different alpha-blockers on the human myofibroblast cell line WPMY-1. Their findings indicate that cytotoxicity is time-dependent and that the effects of tamsulosin, alfuzosin, and terazosin are not significant up to a concentration of 100 µM, resulting in a reduction in viability of more than 50%.[32] In a review by Batty et al. (2016), it is concluded that tamsulosin does not exhibit the cytotoxic effects seen with other alpha-blockers on prostate cancer cell lines (PC-3, LNCaP, and DU-145). Once again, the cytotoxic effects of doxazosin, terazosin, and prazosin are attributed to the quinazoline ring, while in naftopidil, it's the piperazine ring, with tamsulosin being an alpha-blocker with the chemical identity of a sulfonamide.[32] Medina-Pizaño (2022) also reports that lower concentrations of carvedilol resulted in decreased cell viability, while higher concentrations even increased viability, suggesting a proliferative effect.[19]

In our case, we observed a time-dependent negative effect on cell viability. This effect may be associated with the constitutive function of adrenergic receptors in hepatocytes, which play a role in modulating several functions such as carbohydrate, lipid, and amino acid metabolism.[34] Type 1 adrenergic receptors are involved in liver regeneration and glycogenolysis,[35] while beta receptors (predominantly types 1 and 2) regulate liver glucose disposal and lipid catabolism similarly to glucagon. Additionally, the activation of hormone-sensitive lipase (HSL) and adipocytic triglyceride lipase (ATGL) is also stimulated.[36]

Another explanation for the cytotoxicity observed with adrenergic blockers over longer interaction times could be the generation of reactive metabolites resulting from their biotransformation in the liver via CYP P450. This hypothesis is one of the most plausible explanations for the etiopathogenesis of drug-induced hepatotoxicity. During the detoxification process of xenobiotics, free radicals and compounds that covalently bind to lipids, nucleic acids, or proteins can be generated.[37] Several case studies support this hypothesis for carvedilol[38–40]; however, information on tamsulosin is more limited.

Following this line of reasoning, the specific binding of reactive metabolites with macromolecules such as proteins is termed haptenization.[18] It is one of the described mechanisms of hepatotoxicity and represents an idiosyncratic reaction because its effects are not related to the therapeutic effect or dose of the drug. Additionally, it primarily induces cellular-level liver failure.[41]

Thus, secondary metabolites produced by the CYP P450 system can affect the ER membrane of hepatocytes, binding to proteins, causing changes in their conformation. These changes may eventually be recognized by the quality control system, leading to a potential response to misfolded proteins. This mechanism's significance lies in its association with diseases such as hepatitis, alcoholic liver disease, and fatty liver disease.[20] Hepatocyte apoptosis is a common pathogenic event in several liver diseases and is linked to unresolved ER stress.[42] However, the extent to which reactive metabolites activate the UPR is not clearly understood, and there is limited evidence supporting this.[41]

Our findings indicate that the mRNA expression of the PERK-ATF4 branch is partially activated during treatments with carvedilol and tamsulosin. Once PERK is activated, it leads to a reduction in global protein synthesis, which is a result of eIF2 phosphorylation and promotes mRNA translation with a regulatory signal in the 5' non-coding region

(UTR) like ATF4[43] However, the analysis of puromycylated peptides reveals that there are no statistically significant differences in the rate of protein synthesis, even though there is a downward trend in the group treated with carvedilol.

The branch of the UPR mediated by IRE1α was partially activated at the mRNA level in the case of both adrenoblockers. Haas et al. (2016) induced endoplasmic reticulum stress using high concentrations of dextrose in HCAEC cells[44] and subsequently treated them with beta-blockers (carvedilol, propranolol, and atenolol). They concluded that these beta-blockers can suppress the cellular UPR since there was a decrease in the expression of GRP78, phosphorylation of eIF2, JNK, and XBP1 splicing. It's worth noting that these effects were observed at concentrations up to 10 µM,[45] whereas our studies used lower concentrations. The studies by Gao et al. (2017) also suggest that carvedilol has a regulatory effect on the expression of this branch of the UPR.

In our findings, we observed an overexpression of GRP78 at the messenger RNA level; however, no significant differences were observed in protein synthesis. It's important to note that, apart from being an endoplasmic reticulum chaperone protein that facilitates the folding process, GRP78 also functions as a sensor of endoplasmic reticular stress.[46] This leads us to believe that both tamsulosin and carvedilol do not induce severe endoplasmic reticulum stress, or at least do so to a very limited extent, and can be managed by the cell within the first 24 hours of interaction.

On other hand, one of the signaling pathways related to the UPR is autophagy, as misfolded polypeptides can aggregate to form aggregates (aggregasomes) and amyloid fibers.[47,48] In these cases, additional signaling pathways, such as autophagy, are activated. There is evidence suggesting that autophagy plays a role in post-stress survival in the ER but can also trigger apoptosis, as they share some upstream signals.[49] However, the synthesis rate of LC3-II/LC3-I proteins indicates that there is no formation of autophagosomes.

CONCLUSION

Carvedilol and tamsulosin treatments at serum concentrations stimulate partial activation of the UPR at the transcriptional level, which probably responds to drug-induced stress, specifically in the IRE1α-XBP1 and PERK-ATF4 branches. However, there is no significant expression of the molecular chaperone GRP78 or its effector signaling pathways. Therefore, it is assumed that the interaction of hepatocytes with carvedilol and tamsulosin is stable and does not affect the integrity of the endoplasmic reticulum.

ACKNOWLEDGMENTS

LAQB Cintya Esquivel-Dueñas and LAQB Mariana Perez-Villalobos, Department of Chemistry, Autonomous University of Aguascalientes, for their excellent technical assistance. JCRN gratefully acknowledges the scholarship granted by CONACYT as part of the master's program in Biomedical Research of the Autonomous University of Aguascalientes.

Funding

This work was supported by INCyTEA under Grant FEIT-2023, CONACYT under Grant 241312 and A1-S-21375 and the Autonomous University of Aguascalientes under Grant PIBB 19-11n.

Availability of data and materials

Data available on request from the authors.

Authors' contributions

MYMP developed cytotoxicity techniques, RT qPCR, the analysis and interpretation of all data. SLMH performed western blot. PBI developed the puromycin assay. DIM, JVJ and MHMO contributed to the study conception, design, writing and revision of the manuscript. All authors read and approved the final manuscript.

Ethics approval and consent to participate

Not applicable.

Patient consent for publication

Not applicable.

Competing interests

The authors report there are no competing interests to declare.

REFERENCES

1. Sorota S. The Sympathetic Nervous System as a Target for the Treatment of Hypertension and Cardiometabolic Diseases. J Cardiovasc Pharmacol, 2014; 63: 466–476. DOI: 10.1097/FJC.0000000000000064.
2. Alcántara-Hernández R and Hernández-Méndez A. Complejos moleculares de la señalización adrenérgica Gaceta Médica de México. Gac Med Mex, 2018; 154: 223–235, DOI://dx.doi.org/10.24875/GMM.18002390.
3. Hieble JP. Adrenergic receptors. In: Encyclopedia of Neuroscience. Squire LR (ed.) Academic Press, Wayne, PA, USA, 2009; pp135–139. doi: 10.3389/fphar.2020.581098.
4. Ford APDW, Daniels D V., Chang DJ, Gever JR, Jasper JR, Lesnick JD and Clarke DE. Pharmacological pleiotropism of the human recombinant α(1A)-adrenoceptor: Implications for α1-adrenoceptor classification. Br J Pharmacol, 1997; 121: 1127–1135.
5. Homma N, Hirasawa A, Shibata K, Hashimito K and Tsujimoto G. Both α(1A)- and α(1B)-adrenergic receptor subtypes couple to the transient outward current (I(To)) in rat ventricular myocytes. Br J Pharmacol, 2000; 129: 1113–1120. DOI: 10.1038/sj.bjp.0703179.
6. Williams TJ, Blue DR, Daniels D V., *et al.* In vitro α1-adrenoceptor pharmacology of Ro 70-0004 and RS-100329, novel α(1A)-adrenoceptor selective antagonists. Br J Pharmacol, 1999; 127: 252–258.
7. Dunn CJ, Matheson A and Faulds DM. Tamsulosin: A review of its pharmacology and therapeutic efficacy in the management of lower urinary tract symptoms. Drugs and Aging, 2002; 19: 135–161. DOI: 10.2165/00002512-200219020-00004.
8. Mctavish D, Campoli-richards D and Sorkin EM. (1993). Carvedilol Therapeutic Efficacy. Drugs 45: 232–258.
9. Keating GM and Jarvis B: Carvedilol. (2003). A review of its use in chronic heart failure. Drugs 63: 1697–1741. DOI: 10.2165/00003495-200363160-00006.
10. Pose E and Cardenas A. Translating Our Current Understanding of Ascites Management into New Therapies for Patients with Cirrhosis and Fluid Retention, Dig Dis, 2017; 35: 402–410. DOI: 10.1159/000456595.
11. Kockerling D, Rooshi Nathwani, Forlano R, Manousou P, Mullish BH, Dhar A. Current and future pharmacological therapies for managing cirrhosis and its complications. World J Gastroenterol, 2019; 25: 888–908. doi: 10.3748/wjg.v25.i8.888.
12. Oben JA and Diehl AM. Sympathetic nervous system regulation of liver repair. Anat Rec - Part A Discov Mol Cell Evol Biol, 2004; 280: 874–883. DOI: 10.1002/ar.a.20081.

13. Gao P, Yang B, Yu HY, Meng RR and Si JY. Carvedilol alleviates the biliary cirrhosis through inhibiting the endoplasmic reticulum stress. Eur Rev Med Pharmacol Sci, 2017; 21: 5813–5820. DOI: 10.26355/eurrev_201712_14029.
14. De Araújo RF, Garcia VB, De Carvalho Leitão RF, De Castro Brito GA, De Castro Miguel E, Guedes PMM and De Araújo AA. Carvedilol improves inflammatory response, oxidative stress and fibrosis in the alcohol-induced liver injury in rats by regulating kuppfer cells and hepatic stellate cells. PLoS One, 2016; 11: 1–23. DOI: 10.1371/journal.pone.0148868.
15. Serna-Salas SA, Navarro-González YD, Martínez-Hernández SL, *et al.* Doxazosin and Carvedilol Treatment Improves Hepatic Regeneration in a Hamster Model of Cirrhosis. Biomed Res Int: 2018; 1–11. DOI: 10.1155/2018/4706976.
16. Macías-Pérez JR, Vázquez-López BJ, Muñoz-Ortega MH, Aldaba-Muruato LR, Martínez-Hernández SL, Sánchez-Alemán E and Ventura-Juárez J. Curcumin and α/β-Adrenergic antagonists cotreatment reverse liver cirrhosis in hamsters: Participation of Nrf-2 and NF-κB. J Immunol Res 2019; 1–12. doi: 10.1155/2019/3019794.
17. Rodríguez González JC and Rodeiro Guerra I. El sistema citocromo p450 y el metabolismo de xenobióticos. Rev Cuba Farm, 2014; 48: 495–507.
18. Gunawan BK and Kaplowitz N. Mechanisms of Drug-Induced Liver Disease. Clin Liver Dis, 2017; 11: 459–475. DOI: 10.1016/j.cld.2007.06.001.
19. Medina-pizaño MY, Medina-rosales MN, Martínez-hernández SL, *et al.* Protective Effect of Curcumin against Doxazosin- and Carvedilol- Induced Oxidative Stress in HepG2 Cells. Oxid Med Cell Longev, 2022: 15. DOI: 10.1155/2022/6085515.
20. Chen S, Melchior, W. B. J and Guo L. Endoplasmic Reticulum Stress in Drug- and Environmental Toxicant-Induced Liver Toxicity. J Env Sci Heal C Env Carcinog Ecotoxicol, 2014; 32: 83–104. DOI: 10.1080/10590501.2014.881648.
21. Szegezdi E, Logue SE, Gorman AM and Samali A. Mediators of endoplasmic reticulum stress-induced apoptosis. EMBO Rep, 2006; 7: 880–885. DOI: 10.1038/sj.embor.7400779.
22. Hipp MS, Kasturi P and Hartl FU. The proteostasis network and its decline in ageing. Nat Rev Mol Cell Biol, 2019; 20: 421–435. DOI: 10.1038/s41580-019-0101-y.
23. Bravo R, Parra V, Gatica D, *et al.* Endoplasmic Reticulum and the Unfolded Protein Response: Dynamics and Metabolic Integration. Int Rev Cell Mol Biol, 2013; 301: 210–290, 2013. DOI: 10.1016/B978-0-12-407704-1.00005-1.
24. Hetz C and Papa FR. The Unfolded Protein Response and Cell Fate Control. Mol Cell, 2018; 69: 169–181. DOI: 10.1016/j.molcel.2017.06.017.
25. Abdullahi A, Stanojcic M, Parousis A, Patsouris D and Jeschke MG. Modeling ER Stress In Vitro and In Vivo. Shock, 2017; 47: 506–513. DOI: 10.1097/SHK.0000000000000759.
26. Benson DA, Cavanaugh M, Clark K, Karsch-Mizrachi I, Lipman DJ, Ostell J and Sayers EW. GenBank. Nucleic Acids Res, 2013; 41: 36–42.
27. Ye J, Coulouris G, Zaretskaya I, Cutcutache I, Rozen S and Madden TL. Primer-BLAST: A tool to design target-specific primers for polymerase chain reaction. BMC Bioinformatics, 2012; 13: 11. DOI: 10.1186/1471-2105-13-134.
28. Schmittgen TD and Livak KJ. Analyzing real-time PCR data by the comparative CT method. Nat Protoc, 2008; 3:

1101–1108. DOI: 10.1038/nprot.2008.73.

29. Ravi V, Jain A, Mishra S and Sundaresan NR. Measuring Protein Synthesis in Cultured Cells and Mouse Tissues Using the Non-radioactive SUnSET Assay. Curr Protoc Mol Biol, 2020; 133: 1–23. DOI: 10.1002/cpmb.127.
30. Kim YH, Choi HY, Noh YH, Lee SH, Lim HS, Kim C and Bae KS. Dose proportionality and pharmacokinetics of carvedilol sustained-release formulation: A single dose-ascending 10-sequence incomplete block study. Drug Des Devel Ther, 2015; 9: 2911–2918. DOI: 10.2147/DDDT.S86168.
31. Forbes A, Anoopkumar-Dukie S, Chess-Williams R and McDermott C. Relative cytotoxic potencies and cell death mechanisms of α1-adrenoceptor antagonists in prostate cancer cell lines. Prostate, 2016; 76: 757–766. DOI: 10.1002/pros.23167.
32. Batty M, Pugh R, Rathinam I, *et al.* The role of α1-adrenoceptor antagonists in the treatment of prostate and other cancers. Int J Mol Sci, 2016; 17: 1–25. doi: 10.3390/ijms17081339.
33. Iwamoto Y, Ishii K, Sasaki T, *et al.* Oral naftopidil suppresses human renal-cell carcinoma by inducing G 1 cell-cycle arrest in tumor and vascular endothelial cells. Cancer Prev Res, 2013; 6: 1000–1006, 2013. DOI: 10.1158/1940-6207.CAPR-13-0095.
34. Exton JH. Mechanisms involved in α-adrenergic phenomena: Role of calcium ions in actions of catecholamines in liver and other tissues. Am J Physiol - Endocrinol Metab, 1980; 1: 3–12.
35. Cruise JL, Knechtle SJ, Bollinger R, Kuhn C and Michalopoulos G. α1-Adrenergic Effects and Liver Regeneration. Hepatology, 1987; 7: 1189–1194. DOI: 10.1002/hep.1840070604.
36. Kimura T, Pydi SP, Pham J and Tanaka N. Metabolic functions of g protein-coupled receptors in hepatocytes—potential applications for diabetes and nafld. Biomolecules, 2020; 10: 1–16. DOI: 10.3390/biom10101445.
37. Tejada F. Hepatotoxicidad por farmacos. Rev Clínica Med Fam, 2010; 3: 177–191. DOI:10.4321/S1699-695X2010000300006
38. NIH. (2017). Carvedilol. Bethesda, MD.
39. Hagmeyer KO and Stein J. Hepatotoxicity associated with carvedilol. Ann Pharmacother, 2001; 35: 1364–1366. DOI: 10.1345/aph.10239
40. Rua J, Prata AR, Marques R, Silva R, Gomes B, Fraga J and Fortuna J. Carvedilol-Induced Liver Injury, a Rare Cause of Mixed Hepatitis: A Clinical Case. GE Port J Gastroenterol, 2019; 26: 196–201. DOI: 10.1159/000490205
41. Uetrecht J. Mechanisms of idiosyncratic drug-induced liver injury. In: Advances in Pharmacology, 1th ed. vol. 85 Ramachandran A and Jaeschke H (eds.) Academic Press, KS, 2019; pp133–163. DOI: 10.1016/bs.apha.2018.12.001
42. Malhi H and Kaufman RJ. Endoplasmic reticulum stress in liver disease. J Hepatol, 2011; 54: 795–809. DOI: 10.1016/j.jhep.2010.11.005
43. Scheper GC, Van Der Knaap MS and Proud CG. Translation matters: Protein synthesis defects in inherited disease. Nat Rev Genet, 2007; 8: 711–723. DOI: 10.1038/nrg2142.
44. Sheikh-ali M, Sultan S, Alamir A, Haas MJ and Mooradian AD. Hyperglycemia-induced endoplasmic reticulum stress in endothelial cells. Nutrition, 2010; 26: 1146–1150. DOI: 10.1016/j.nut.2009.08.019.
45. Haas MJ, Kurban W, Shah H, Onstead-Haas L and Mooradian AD. Beta blockers suppress dextrose-induced endoplasmic reticulum stress, oxidative stress, and apoptosis in human coronary artery endothelial cells. Am J Ther, 2016; 23: e1524–e1531. DOI: 10.1097/MJT.0000000000000200.
46. Kopp MC, Larburu N, Durairaj V, Adams CJ and Ali MMU UPR proteins IRE1 and PERK switch BiP from

chaperone to ER stress sensor. Nat Struct Mol Biol, 2019; 26: 1053–1062. DOI: 10.1038/s41594-019-0324-9.

47. Klaips CL, Jayaraj GG and Hartl FU. Pathways of cellular proteostasis in aging and disease. J Cell Biol, 2018; 217: 51–63. DOI: 10.1083/jcb.201709072.
48. Kim YE, Hipp MS, Bracher A, Hayer-Hartl M, Hartl FU. Molecular chaperone functions in protein folding and proteostasis. Annu Rev Biochem, 2013; 82:323-55. doi: 10.1146/annurev-biochem-060208-092442.
49. Shuling S, Jin T, Yuyang M, Mengmeng L and Qiang Z. Crosstalk of autophagy and apoptosis: involvement of the dual role of autophagy under ER stress. J Cell Physiol, 2017; 232: 2977–2984. DOI: 10.1002/jcp.25785.